ELSEVIER

Journal of Nuclear Materials 244 (1997) 66–74

journal of nuclear materials

Oxidation and dissolution of nuclear fuel (UO_2) by the products of the alpha radiolysis of water

S. Sunder *, D.W. Shoesmith, N.H. Miller

Atomic Energy of Canada Limited, Whiteshell Laboratories, Pinawa, Man., Canada ROE 1L0

Received 2 April 1996; accepted 13 September 1996

Abstract

Oxidation of UO_2 nuclear fuel by the products of the alpha radiolysis of water has been measured as a function of strength of the alpha flux and solution pH (0.1 mol L^{-1} $NaClO_4$, $3.5 \leq pH \leq 11$) using electrochemical techniques. Corrosion potentials were measured using a thin-layer corrosion cell in which an alpha source was brought within 30 μm of a UO_2 electrode. Oxidative dissolution (corrosion) rates were then calculated as a function of alpha dose rate from the steady-state values of the corrosion potential using an electrochemical model. The corrosion rate was found to increase with an increase in alpha dose rate and with a decrease in pH for values < 4. A procedure to predict the corrosion rate of used nuclear fuel in groundwater as a function of fuel cooling time is then described. As a consequence of the cell geometry used in corrosion potential measurements these predicted rates are appropriately applied to dissolution in cracks and fissures. The corrosion of fuel, supported solely by the alpha radiolysis of water, is predicted to be unimportant for CANDU reactor fuel with a burnup of 685 GJ/kg U for periods ≥ 600 a. However, for fuel with higher burnups, e.g., a typical PWR fuel (burnup 3888 GJ/kg U (45 MW d/kg U)), corrosion supported by the alpha radiolysis of water could be significant for time periods of ~ 2000 a. For periods greater than this (~ 600 a (CANDU); ~ 2000 a (PWR)) the oxidative dissolution can be appropriately considered as a chemical as opposed to corrosion reaction.

1. Introduction

The concept of direct disposal of used nuclear fuel in a geological disposal vault is being considered in several countries, including Canada, Sweden and the USA [1–15]. Transport by groundwater is the only credible mechanism for the migration of radionuclides contained in the used-fuel bundles in the disposal vault to the biosphere. Used fuel is largely UO_2 with only a small fraction of other actinides and fission products. A great majority ($> 95\%$) of these radionuclides are dispersed or in solid solution in the UO_2 matrix [1]. Hence, dissolution of UO_2 is a major potential pathway for the release of radionuclides contained within used fuel and the evaluation of a disposal concept requires a knowledge of the dissolution rate of the fuel.

The dissolution rate of UO_2 in aqueous environments depends on the degree of surface oxidation of the fuel, which is governed by the solution redox conditions [4,12,15–17]. Although the groundwaters at the planned depth of the disposal vault in the Canadian nuclear fuel waste management program (CNFWMP), 500–1000 m, are generally reducing [18] [1], the redox conditions of the groundwater coming into contact with the used fuel can be made oxidizing by the dissolution of oxygen trapped within the vault on sealing [12] or by the radiolysis of water by the ionizing radiation associated with the used fuel [2–5]. The dissolved oxygen trapped on vault closure will be consumed by corrosion of the container and by reaction with iron-containing clays, minerals and oxidizable organic material, and may be consumed in a few tens of years [19].

* Corresponding author. Tel.: +1-204 753 2311; fax: +1-204 753 2455; e-mail: sunders@aecl.ca.

[1] Report available from SDDO, AECL Research, Chalk River Laboratories, Chalk River, Ont., Canada K0J 0J0.

PII S0022-3115(96)00709-X

Providing that the container survives this oxidizing period, no dissolved oxidants will enter the container when it eventually does fail. The products of water radiolysis, however, will be available at the fuel surface as soon as it comes in contact with the groundwater, and their ability to sustain oxidizing conditions will be related to the dose rate and its rate of decay with time [20–22].

The strong beta and gamma radiation fields associated with fuel will decrease by a factor $>10^3$ in several hundred years, whereas the alpha fields, although initially much weaker, will persist for a much longer period of time [20,21]. Since the range of the alpha particle in water is short [2,21,23,24], radiolysis leading to oxidative dissolution (corrosion) is most likely to occur in wet cracks in the fuel or at waterlogged sites within the cladding gap, where loss of the molecular oxidants by diffusive transport is likely to be slow. For Grade-2 titanium containers, one of the container materials being considered in Canada, a conservative model, based on failure by crevice corrosion and hydrogen-induced cracking, predicts failure between 1200 and 7000 a [13,25]. Consequently, it is possible that significant alpha fields could persist beyond the predicted lifetimes of these containers.

Presently available used fuels are generally <30 a old and, consequently have high gamma/beta fields. Their use, therefore, to study the effects of alpha radiolysis on fuel dissolution and radionuclide release is limited. In this paper we describe an experimental strategy for determining fuel dissolution rates as a function of alpha source strength which is free from the interferences from beta/gamma effects. The results obtained are then used to predict the alpha radiolysis effects as a function of emplacement time of the waste in the vault.

2. Chemistry of UO_2 dissolution

Fig. 1 shows the expected composition of a UO_2 surface as a function of the corrosion potential (E_{CORR}) achieved in aqueous solutions (pH ~ 9.5) at room temperature. The compositions indicated were established by a combination of electrochemical, corrosion, and X-ray photoelectron spectroscopic techniques (XPS) [4,5,26,27]. The behavior of the UO_2 surface has been divided into three distinct regions. At very low potentials ($E_{CORR} \leq -400$ mV (versus saturated calomel electrodes, SCE), region 3), no oxidative dissolution of the fuel can be detected, even by techniques as sensitive as photothermal deflection spectroscopy (PDS) [28]. Consequently, it cannot be determined whether oxidative dissolution ($U^{IV}O_2(solid) \rightarrow U^{VI}O_2^{2+}(solution)$) or whether chemical dissolution ($U^{IV}O_2(solid) \rightarrow U^{4+}(solution)$) predominates. For -400 mV $\leq E_{CORR} \leq -100$ mV (versus SCE), region 2 in Fig. 1, the surface composition and extent of oxide formation are directly determined by the potential achieved during natural corrosion [29–31] or applied electrochemically. To sustain the potential within this range under natural corrosion conditions requires only very small concentrations of oxidants (i.e., a low redox potential, E_h) and the potential driving force for oxidative dissolution will be very small (i.e., $E_h \sim E_{CORR}$) [15]. Although PDS results show that dissolution is oxidative in character at potentials as low as -300 mV (versus SCE) [28], it is reasonable to assume that a state close to redox equilibrium is achieved at the fuel/solution interface. Electrochemical and XPS evidence in support of this argument have been published elsewhere [32]. For these conditions, providing diffusive transport is slow, as expected in a waste vault, it is appropriate to apply a solubility-based, transport-limited model to describe the dissolution behavior of the fuel, Fig. 1.

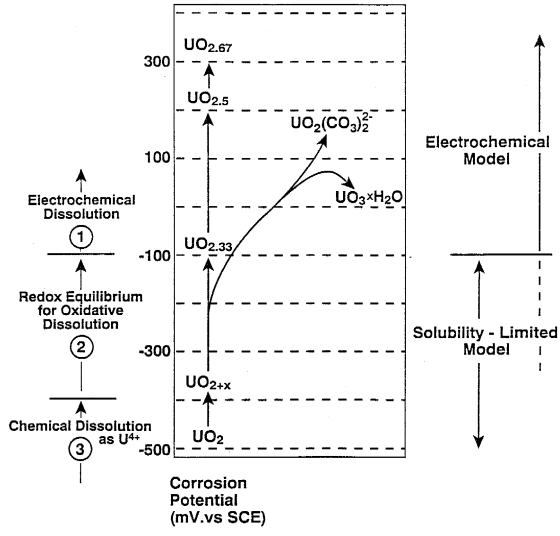

Fig. 1. Surface chemistry of UO_2 as a function of the corrosion potential (E_{CORR}) in near-neutral aqueous solutions.

When $E_{CORR} \geq -100$ mV (versus SCE), region 1 in Fig. 1, redox conditions are sufficiently oxidizing that the oxidative dissolution reaction must be treated as a kinetic corrosion process (i.e., $E_h > E_{CORR}$). For very positive potentials, achievable with applied electrochemical potentials (>200 mV (versus SCE)), the fuel surface may recrystallize to $UO_{2.67}$ [4,26]. Although XPS results suggest this is possible at room temperature under electrochemical conditions, its occurrence at higher temperatures (≥ 150°C) is well documented under hydrothermal [33] or radiolytic oxidizing conditions [34]. Simultaneously, dissolution as UO_2^{2+} occurs and, for solutions in which uranyl species have a low solubility, secondary phases (such as $UO_3 \cdot 2H_2O$) precipitate on the electrode surface. In the presence of uranyl complexing anions (such as carbonate), secondary phase formation can be avoided [4].

In this last range ($E_h > E_{CORR}$) oxidative dissolution is an electrochemical coupling of oxide dissolution and oxidant reduction, and we have recently published a proce-

dure for determining rates electrochemically [5,7]. Electrochemical dissolution currents measured at positive applied potentials obey the Tafel relationship and can be extrapolated to values of E_{CORR} measured in solutions containing various concentrations of oxidants [5,7,29,35]. In this manner, the dissolution rate of UO_2 fuel can be obtained as a function of oxidant concentration. The extension of this procedure to develop a mixed potential model for fuel dissolution is underway, but incomplete.

3. Experimental

Electrodes constructed from unirradiated CANDU fuel (UO_2) [26] were exposed to the products of alpha radiolysis of water in a specially designed thin-layer electrochemical cell, similar to that described by Bailey et al. [24]. This cell allows measurement of E_{CORR} of a UO_2 electrode as a function of its distance from an alpha radiation source. Most of the studies presented here were conducted at a separation of 30 μm, a distance approximately equal to the mean free path of the alpha particle in water [21,24].

The cell was placed in an oxygen-free, nitrogen-purged anaerobic chamber to minimize oxidation of the UO_2 electrode by atmospheric oxygen. Experiments were performed in 0.1 mol L^{-1} $NaClO_4$ solution purged with high-purity argon for ≥ 30 min to remove the last traces of dissolved oxygen. (The concentration of oxygen in the purge gas was < 1 μg g^{-1}.) During an experiment an argon purge was maintained over the solution. In the majority of experiments the pH was established at 9.5, a value typical of that expected in groundwaters. In a few experiments the pH was adjusted to other values using either $HClO_4$ or NaOH solutions. Solutions of lower pH were used to simulate the potentially acidic 'crevice' chemistry conditions, which could possibly arise in a crack in wet used fuel. The pH was also measured on completion of the experiment.

A freshly polished UO_2 electrode was cathodically cleaned at a potential of -2.0 V (versus SCE) for 5 min. This procedure was conducted with a separation of ~ 660 μm between the electrode and the alpha source, and ensured that the UO_2 surface was fully reduced before exposure to the products of alpha radiolysis. Subsequently, the electrode was brought close to the alpha source (to a separation of 30 μm) and E_{CORR} was measured as a function of time for periods ≥ 6 d.

The alpha sources were circular disks of diameter 1.6 cm and were obtained from NRD (Grand Island, NY). The alpha particle energies were measured at the Whiteshell Laboratories. Two types of gold-plated alpha sources were used: ^{210}Po ($t_{1/2} = 138$ d) with an average alpha particle energy of 4.0 MeV (literature value 5.30 MeV [36]); and ^{241}Am ($t_{1/2} = 432$ a), with an average alpha particle energy of 4.7 MeV (literature value 5.486 MeV [36]). The measured energies are lower than the literature values due to the attenuation of the alpha-particle energies by the gold coating. The ^{210}Po sources had initial activities of 1000 and 100 μCi and the ^{241}Am sources had activities of 400, 250 and 50 μCi, respectively (1 μCi = 3700 Bq).

4. Results and discussion

A large number of experiments were carried out with pH = 9.5, the pH at which the dissolution currents used in our electrochemical model were measured [5]. Fig. 2 shows E_{CORR} as a function of time of exposure to ^{210}Po alpha sources of activity 428 and 55 μCi, respectively. The E_{CORR} versus t profiles have the same general shape observed for oxidation in the presence of molecular oxidants (O_2, H_2O_2) [29,30,35] and oxidants produced by the gamma radiolysis of water [11]. The value of E_{CORR} for the UO_2 electrode facing the higher activity alpha source rises rapidly through regions 3 and 2 to achieve a steady-state value ($(E_{CORR})_{SS}$) in region 1 after ~ 9000 min (6 d). E_{CORR} for the lower strength source rises more slowly and is only just approaching a steady state in region 2 after 6 d.

We have used two parameters to interpret the significance of these E_{CORR} versus t profiles:

(i) the reciprocal of the time to achieve a value of -100 mV (versus SCE), t_{-100}, is an indication of the rate of oxidation of UO_2 to UO_{2+x} (up to $\sim UO_{2.33}$) [3] in region 2;

(ii) the value of $(E_{CORR})_{SS}$ can be used in our electrochemical model to predict the oxidative dissolution (corrosion) rate of the fuel [5].

The values of $(t_{-100})^{-1}$ obtained are plotted as a function of alpha source strength in Fig. 3. These values of t_{-100} are much larger than those recorded in aerated solutions [29–31] or in solutions containing chemically-ad-

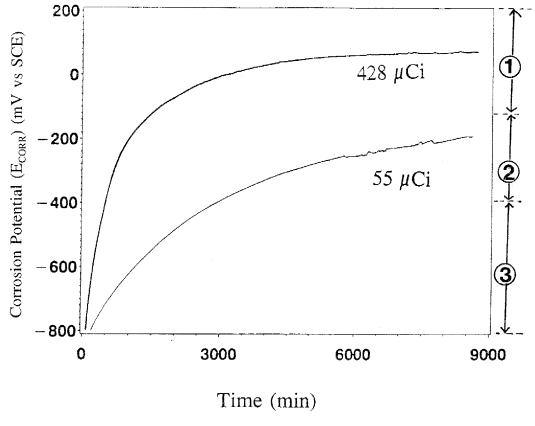

Fig. 2. Open-circuit corrosion potential (E_{CORR}) as a function of time for UO_2 electrodes facing ^{210}Po alpha sources at a separation of 30 μm in a thin-layer cell containing, 0.1 mol L^{-1} $NaClO_4$ solution, pH = 9.5; (a) source strength, 428 μCi; and (b) source strength, 55 μCi (1 μCi = 3700 Bq). See Fig. 1 for the explanation of the three regions indicated on the right hand Y-axis.

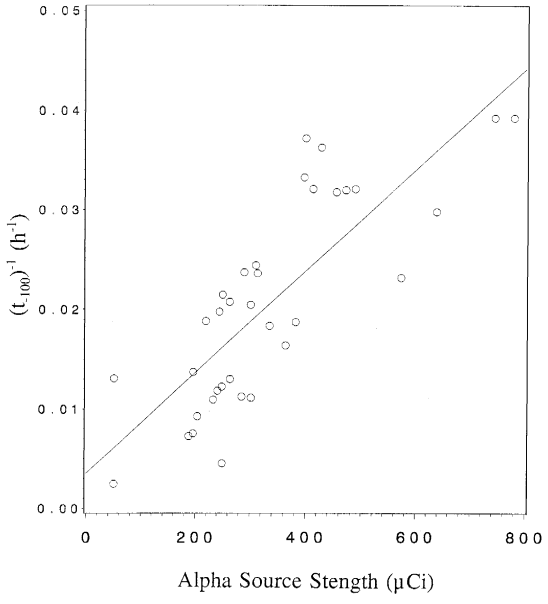

Fig. 3. The reciprocal of the time for E_{CORR} to achieve a value of −100 mV (versus SCE), t_{-100}, as a function of the alpha-source strength used in the experiments.

ded H_2O_2 [35]. For an electrode facing a 250 μCi source, t_{-100} is in the range 35 to 50 h compared with ~3 to 6 h for aerated unirradiated solutions. This slow change in E_{CORR} is most probably due to the slow buildup of alpha radiolysis products at the electrode surface. This buildup will be slowed by diffusive losses at the perimeter of the thin disc of solution separating the electrode and the source. Previous experiments in which the gap was opened and closed a number of times during the experiment showed that E_{CORR} did respond to decreases (after opening) and increases (after closing) in the concentration of oxidants in the gap [24]. The fall in E_{CORR} from the steady-state value on opening the gap was instantaneous, suggesting that $(E_{CORR})_{SS}$ is sustained by a redox reaction involving the radiolytic oxidants. A similar response of E_{CORR} to the addition or removal of chemically added H_2O_2 in the absence of radiolysis [37] suggests $(E_{CORR})_{SS}$ is established by a redox reaction involving this oxidant produced by the alpha radiolysis of the water. The much slower increase in E_{CORR} on reestablishing the 30 μm gap is a clear indication that the potential of the electrode is responding to the buildup of radiolysis products.

There appears to be a first-order relationship between the rate of UO_2 oxidation ($\propto (t_{-100})^{-1}$) and the source strength, Fig. 3. (The fitted line is described by the equation $y = mx + a$, where $y = 1/t_{-100}$, $x = \mu Ci$, $m = 5.08(\pm 0.67) \times 10^{-5}$ and $a = 3.52(\pm 2.46) \times 10^{-3}$). Since alpha dose rate is directly proportional to the alpha-source strength (Appendix A), we have a first-order relationship between the rate of UO_2 oxidation ($\propto (t_{-100})^{-1}$) and the alpha dose rate. It may be noted here, that for gamma radiolysis we have shown a linear relationship between $(t_{-100})^{-1}$ and *the square root* of dose rate [3], which can be explained by the fact that the steady-state concentrations of radical oxidants, the main oxidants formed during gamma radiolysis, are proportional to the square root of dose rate [3]. Also, it has been shown that it is the concentrations of radicals formed *near* the fuel surface (i.e., within a water layer of thickness equal to the diffusion range of the radicals) that governs the oxidation rates during gamma radiolysis. Transport of radicals from the bulk of solution does not play a significant role in fuel oxidation [38]. However, the situation is not so simple in the case of molecular oxidants, which also play a significant role in the fuel oxidation in the case of alpha radiolysis [39].

Fig. 4 shows the steady-state values of corrosion potential (i.e., the potential achieved after 6 d), $(E_{CORR})_{SS}$, as a function of alpha source strengths used in the corrosion experiments. This data was obtained using several different alpha sources and UO_2 electrodes. The $(E_{CORR})_{SS}$ values increase with the alpha source strength at lower alpha strengths, and reach a limiting value of about 100 mV (versus SCE). The results given in this figure show, that for the UO_2 electrodes facing alpha sources of strength ~100 μCi, $(E_{CORR})_{SS}$ values are less positive than −100 mV, the threshold below which a kinetic model for oxida-

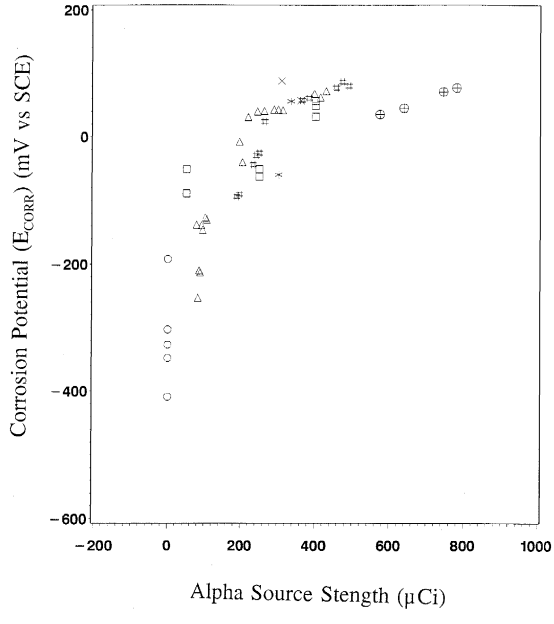

Fig. 4. Steady-state values of open-circuit corrosion potential ($(E_{CORR})_{SS}$) as a function of alpha source strength for UO_2 electrodes facing alpha sources at a separation of 30 μm in a thin-layer cell containing 0.1 mol L^{-1} $NaClO_4$ solution, pH = 9.5; ^{241}Am alpha sources, □; ^{210}Po sources, ∗, #, △, and ⊕; No source (Ar Purge only), ○.

tive dissolution based on electrochemical principles is no longer essential [32].

Fig. 5 shows E_{CORR} versus t plots recorded at pH values of 3.5, 9.5 and 11.0 for a ^{241}Am source of strength 250 μCi. In these experiments the values of t_{-100} were only marginally different for pH = 3.5 and 9.5. The value of 30 to 40 h for t_{-100} should be compared with the value of only a few minutes for oxidation to this stage in aerated and H_2O_2-containing solutions at a similar pH [30,35,37]. (The rapid rises in E_{CORR} to −100 mV (versus SCE) in aerated solutions were possible because the 'slower oxidation step' of UO_2 to $UO_{2.33}$ does not occur at the low pH [30]). The slow response (i.e., high value of t_{-100}), even at pH = 3.5, indicates that although the rate of production of radiolytic oxidants is rapid, it is the increase in the concentration of molecular oxidants that is of primary importance in determining the rate of fuel oxidation during alpha radiolysis. At pH = 11.0, t_{-100} is greater than at pH = 9.5, consistent with a more extensive surface oxidation process before the establishment of steady-state dissolution conditions. Beyond $E_{CORR} = -100$ mV (versus SCE), the approach to steady state is about the same for all three values of pH despite the fact that surface oxidation is expected to be extensive at 9.5 and 11.0 but not at 3.5 [4,15,30]. Again, this is consistent with the rate of potential response being determined predominantly by the rate of radiolytic production of oxidants.

The pH on completion of these three experiments did not differ substantially from the initial set value. However, this was generally not the case for experiments conducted in the range $4 \leq pH \leq 6$, for which the final pH value was

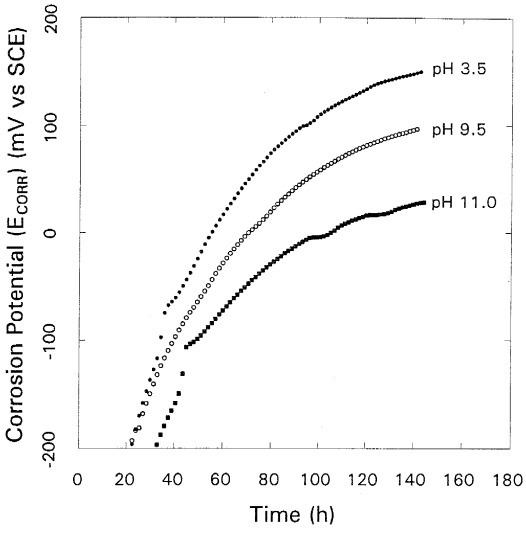

Fig. 5. Open-circuit corrosion potential, E_{CORR}, as a function of time for UO_2 electrodes facing a ^{241}Am alpha source, strength 250 μCi, at a separation of 30 μm in a thin-layer cell containing 0.1 mol L^{-1} $NaClO_4$ solution with: (a) pH = 3.5; (b) 9.5; and (c) pH = 11 (1 μCi = 3700 Bq).

inevitably in the range 7 to 8. There appear to be a number of possible reasons for this pH change:

(i) the radiolysis process in the narrow gap;

(ii) an imbalance in the production of OH^- ions by reduction of H_2O_2 (and possibly also O_2) and its consumption in the hydrolysis of dissolved UO_2^{2+} species including hydroxylation and protonation of the uranium oxide surface; and

(iii) the leaching of basic species from the resin in which the electrode is embedded.

It should be mentioned here that Vochen and De Grave [40] also observed an increase in pH on suspending a powder of pitchblende (a mineral containing uranium oxides, i.e., 53% UO_2, 37% UO_3, 7% Pb oxides, and trace metal oxides) in water. For example, the pH of an aqueous suspension of pitchblende changed from 4 to 7 in about 12 h.

Blank experiments in which only the electrode (set in the resin) alone was exposed to the solution in the absence of any alpha source showed that the whole of the observed pH change could be attributed to leaching of basic species from the resin. The last observation leaves the interpretation of the results at pH = 3.5 in some doubt. Although our measurements show that the pH of the bulk solution did not change substantially, it is possible that the pH within the narrow gap between the electrode and the source was higher than the bulk value. If so, then the E_{CORR} measured will not reflect the expected behavior at pH = 3.5 and will underestimate the effects of a decrease in pH to this value. This makes it difficult to decide what radiolytic oxidant is predominantly involved in establishing the value of E_{CORR} of the UO_2 electrode surface. If E_{CORR} is established by a response to the H_2O_2 then it is expected to change markedly as the pH decreases [37], whereas a response to oxygen would not entail such a marked pH dependence. Unfortunately, the size of the shift in E_{CORR} to more positive values when the pH is changed from 9.5 to 3.5 is smaller than expected for H_2O_2 but greater than expected for O_2 making it difficult to decide which oxidant is predominant.

Predicted corrosion rates are plotted as a function of alpha source strength in Fig. 6. These rates were obtained from the $(E_{CORR})_{SS}$ values and the Tafel slope for anodic dissolution of UO_2 measured as described elsewhere [5]. The horizontal line in Fig. 6, at a corrosion rate of 3×10^{-5} μg cm^{-2} d^{-1}, corresponds to an $(E_{CORR})_{SS}$ value of −100 mV (versus SCE), and represents the boundary between regions 1 and 2 (Figs. 1 and 2). Above this threshold it is necessary to consider fuel dissolution as a corrosion process [32]. For potentials below this threshold, the surface composition becomes potential-dependent and the extrapolation of our electrochemical dissolution currents may not accurately predict dissolution rates. Consequently, the dissolution (corrosion) rate values that fall below this threshold may not represent real values. The two points for low source strengths (~ 50 μCi) that lie

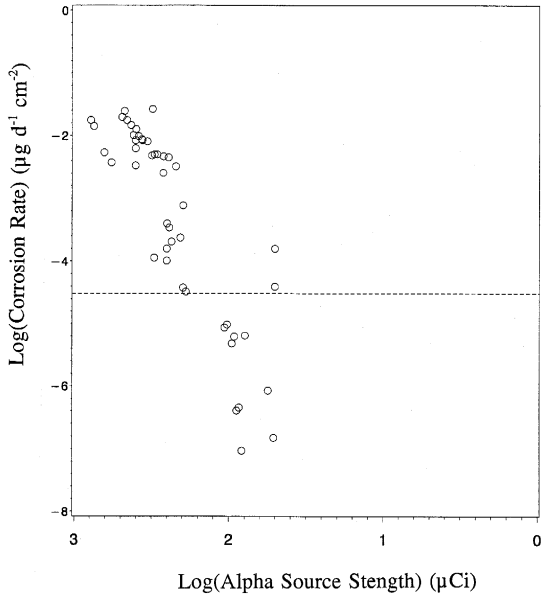

Fig. 6. Corrosion rates of UO_2 as a function of alpha source strength in solutions undergoing alpha radiolysis (0.1 mol L^{-1} $NaClO_4$, pH = 9.5). The horizontal dashed line corresponds to the threshold above which kinetically controlled oxidative dissolution (corrosion) of UO_2 fuel occurs.

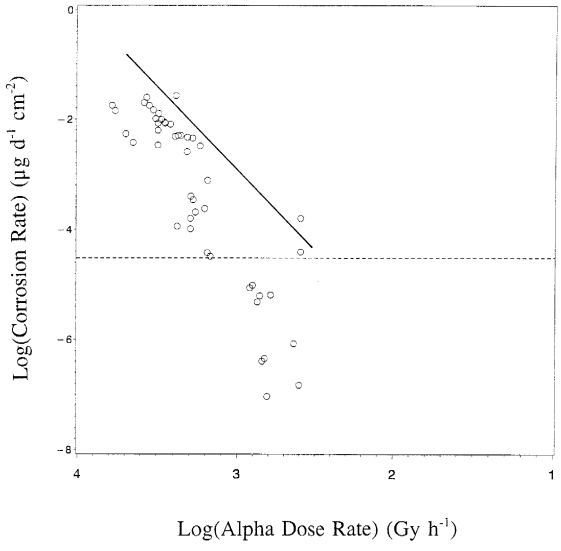

Fig. 7. Corrosion rates of UO_2 as a function of alpha dose rate in solutions undergoing alpha radiolysis (0.1 mol L^{-1} $NaClO_4$, pH = 9.5). The solid line is arbitrarily drawn to encompass all the data points except the two suspiciously high ones at low dose rates.

above this line are suspiciously high and suggest the measurement of E_{CORR} may have been affected by the presence of stray O_2 in these cases. If one were to fit the observed data points (log(corrosion rate) versus log(source strength)) to a straight line, the slope of the line would be ~ 4. Even if one were to drop the points below the horizontal dashed line in Fig. 6 (i.e., the points for which the $(E_{CORR})_{SS}$ is less than -100 mV versus SCE), the slope of the line fitted to the reduced data set would be still greater than 2, that is, the apparent 'reaction order' is substantially > 1. This suggests that we are not observing a simple dissolution rate dependence on alpha source strength. A possible explanation is that the E_{CORR} values are determined by the coupling of H_2O_2 reduction to both the UO_2 oxidative dissolution (corrosion) reaction and to the peroxide decomposition reaction and that the predominantly coupled oxidation reaction changes with source strength.

Fig. 7 shows the corrosion rate as a function of the alpha dose rate in the experiments. Dose rates were calculated following the procedure described in Appendix A. The solid line is arbitrarily drawn to encompass the majority of data points and gives the maximum possible corrosion rates of used fuel as a function of the dose rate. This figure can be used to calculate the fuel corrosion rate caused by alpha radiolysis as a function of age of the fuel (or time in the disposal vault if the fuel is considered to have been emplaced in a waste vault) from a knowledge of the alpha dose rate as a function of fuel age. Recently, alpha dose rates associated with CANDU reactor fuel with a burnup of 685 GJ/kg U have been reported [21]. (This reference also describes a procedure to calculate the alpha dose rate for used CANDU fuel of other burnups as a function of cooling time.) Fig. 8 shows the alpha dose rate for used fuel with a burnup of 685 GJ/kg U as a function of cooling time. It is clear from the results shown in Figs. 7 and 8 that corrosion (oxidative dissolution) supported solely by the alpha radiolysis of water is unimportant at

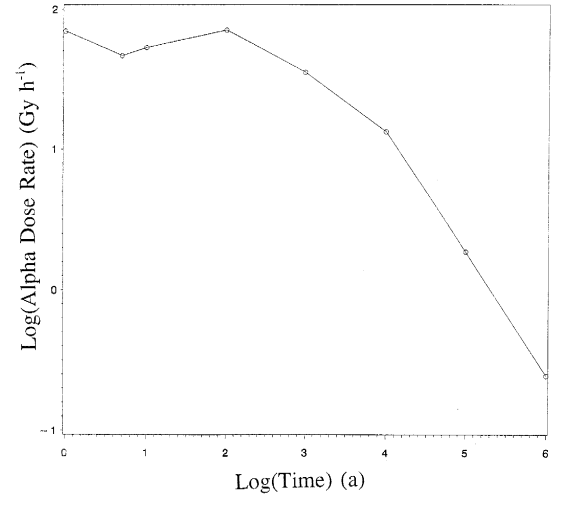

Fig. 8. Alpha dose rate as a function of cooling time in a water layer in contact with used CANDU fuel, burnup of 685 GJ kg^{-1} U (data from Ref. [21]).

long times. The groundwaters at the planned depth of the disposal vault are reducing [18] and the beta and gamma activity associated with the used fuel is significantly reduced after a period of ~ 600 a [20,21], a period shorter than the predicted lifetimes of titanium waste containers (1200 to 7000 a, [12,13,25]). Consequently, the application of a kinetic model for fuel dissolution driven by the products of water radiolysis after container failure is not essential and the presently used solubility-based transport-limited model should be adequate.

A change in the alpha activity of the used fuel, because of different burnup and/or initial composition, affects only the time dependence of the dose rate not the dose rate dependence of the corrosion rate. Therefore, one can calculate the evolution of corrosion behavior with age for any fuel for which the activity (or dose rate) of the fuel as a function of age can be calculated from the results given in Figs. 6 and 7. Fig. 9 shows alpha dose rates in water in contact with PWR fuel with a burnup of 45 MW d kg^{-1} U or 3880 GJ kg^{-1} U (1 MW d = 86.4 GJ) as a function of age. The dose rates used in Fig. 9 were calculated from the alpha dose rate in the fuel using the data of Ingemansson and Elkert [41] and the procedure described elsewhere [21]. Note, the dose rates shown in Figs. 8 and 9 are average values for a water layer of thickness equal to the range of alpha particles (~ 35 μm) in contact with used fuel but outside the fuel. To obtain dose rates in water in small cracks inside the fuel the dose rates shown in Figs. 8 and 9 should be multiplied by a factor of 2 [21,41]. One can conclude from the results given in Figs. 7 and 9, that for PWR fuel with this burnup, corrosion supported by alpha radiolysis could occur over a period of 2000 a. This period for which a kinetic oxidizing model is required would be longer than the predicted lifetimes of most of the titanium containers, and for the solubility-based transport-limited

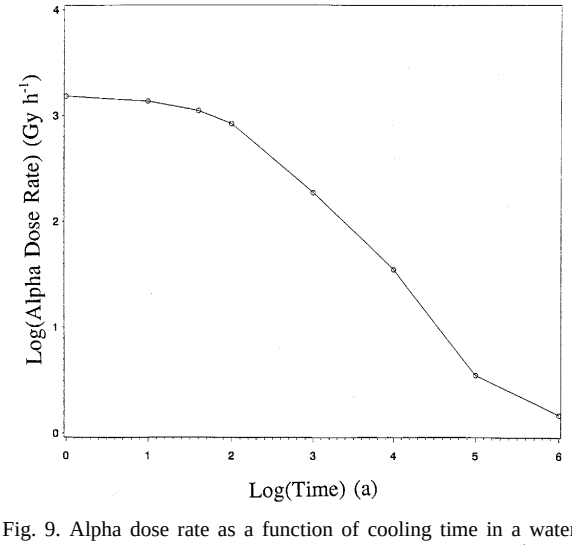

Fig. 9. Alpha dose rate as a function of cooling time in a water layer in contact with PWR used fuel, burnup 45 MW d g^{-1} U.

modelling procedure to remain valid a more durable container would be required. It has been shown elsewhere that much longer periods of containment can be achieved using containers constructed from copper or more crevice-corrosion-resistant titanium alloys [12,13,42,43].

The predictions given here are only valid for the conditions of measurement of the corrosion rates and can only be applied, therefore, to fuel dissolution in non-complexing groundwaters with a neutral to slightly alkaline pH. The presence of carbonate would be expected to increase the corrosion rates, and it would be necessary to use a Tafel relationship for fuel dissolution currents and E_{CORR} values determined in carbonate-containing solution [29]. Also, if the radiolytic oxidant controlling the dissolution of the fuel is H_2O_2, then we might expect the corrosion rate to be dependent on pH and to increase markedly as the pH decreases. We have shown elsewhere that $(E_{CORR})_{SS}$ shifts to much more positive potentials as the pH decreases in H_2O_2-containing solutions [37].

A possible explanation for such a shift in E_{CORR} is that the importance of dissolution, as opposed to H_2O_2 decomposition, increases as the pH falls [37]. One possibility is that locally acidified conditions could be established in areas where occluded chemical conditions could be established; that is within wet cracks and fissures in the fuel. For such a situation to arise the separation of anodic dissolution and oxidant reduction sites associated with localized corrosion processes would be necessary. Whether or not such a situation is possible with used fuel corrosion remains to be demonstrated. Unfortunately, our first attempts to determine whether pH has a significant effect on fuel corrosion driven by alpha radiolysis have proven inconclusive since the actual pH at the corrosion site may not be that set in the bulk of the solution. The E_{CORR} value of ~ 150 mV observed at a set pH = 3.5 suggests that there could be an accelerating effect of a decrease in pH.

The question of the importance of alpha radiolysis under different geometric conditions than those used in these measurements is more difficult to resolve. As a first step we are developing a finite-element model to describe the chemical conditions within the cell gap [44]. In this manner we are attempting to calculate the concentrations of radiolysis products within the gap as a function of alpha source strength. If the dependence of fuel corrosion rate on oxidant concentration can be established, then it should be possible to model the effects of alpha radiolysis for other geometries. Despite these deficiencies the predicted effects of alpha radiolysis presented here can be considered conservative since the concentrations of radiolysis products achievable under less confining geometries (i.e., wider gaps) are expected to be lower [24].

Although it is implicit in our electrochemical model [5,7] that certain amounts of precipitated secondary phases are present on the electrode surface, the possibility that more extensive secondary-phase formation could occur in

natural groundwaters has not been investigated. The presence of secondary phases has been shown to affect corrosion rates [4,45,46]. For the dissolution currents used here (recorded in 0.1 mol L^{-1} $NaClO_4$) the only precipitated phase formed will be $UO_3 \cdot 2H_2O$. In the relatively short experiments to measure E_{CORR}, this phase will be present in only small quantities and may have only a limited blocking effect on the dissolution process. However, the presence of other anions and cations in natural groundwaters could lead to the more extensive formation of very insoluble phases [4,45,47]. If these effects dominate then the predictions of corrosion rates given here will be very conservative.

It should be noted here that the dissolution rates reported are for ambient temperatures. To obtain rates for higher temperatures one would have to multiply the rates reported here with an Arrhenius factor, which would depend upon the activation energy of the oxidative dissolution (corrosion) reaction [4]. Given the chemical complexity of the dissolution reaction there is a strong possibility that such a simple procedure will not suffice [46].

The predictions presented in this paper suggest that the effects of alpha radiolysis on fuel corrosion (dissolution) will be transitory and will become minor as alpha dose rates decrease. Despite the neglect, thus far, of temperature effects and aggressive groundwater constituents (such as carbonate) it does not appear that alpha radiolysis effects will promote extensive fuel corrosion. Although this may be reassuring, it is at odds with more conservative calculations of the extent of fuel oxidation/dissolution based on the assumption that the rate of UO_2 oxidation by alpha radiolysis products will be the same as that of soluble $Fe^{(II)}$ to $Fe^{(III)}$ [48]. That this assumption is suspect is shown by the fact the corrosion (dissolution) rates are higher than those obtained from experiments with used fuel under reducing conditions [48]. (It has been shown that at $\sim$ 100°C the presence of dissolved H_2 (e.g., from the radiolysis of water and/or corrosion of the container and fuel sheath) reduces the oxidation of UO_2 fuel by alpha radiolysis [49].) This discrepancy between our corrosion rate values and those predicted using more conservative models, suggests that not all of the radiolytic oxidants produced lead to corrosion (oxidative dissolution) of the UO_2. Although it is easy to attribute this to the dominance of recombination and decomposition reactions that could be catalyzed by the UO_{2+x} surface, no convincing accounting for the fate of all the oxidants produced radiolytically has yet been performed. A similar discrepancy in the mass balance between radiolytically produced oxidants and the amount of uranium dissolved was reported for the dissolution of irradiated PWR fuel [50].

Acknowledgements

This work is part of the Canadian Nuclear Fuel Waste Management Program, which is jointly funded by AECL and Ontario Hydro under the auspices of the CANDU Owners Group. The authors are grateful to SKB, Stockholm (Sweden) for financial assistance for some of this work, and thank L.H. Johnson and J.C. Tait for helpful comments on the manuscript. AECL #11537, COG#96-34.

Appendix A. Calculation of the alpha dose rate

The alpha dose rate to the UO_2 electrode can be calculated from the geometry of the source, the distance between the source and the electrode and the measured energy of the alpha particle. The surface area of the flat circular source is 2.0 cm^2 (diameter = 1.6 cm). In our experiment the distance between source and electrode was maintained at 30 μm; hence the volume of solution irradiated was 6×10^{-3} cm^3. The average measured energy of the alpha particle is 4.4 MeV (see text) and for a source with a strength of 1 μCi this volume of solution will absorb half of the total number of alpha particles emitted (3.7×10^4 Bq). The other half is emitted from the side of the source not exposed to the solution.

Thus the alpha energy absorbed by the solution in contact with the electrode will be 13.041 erg s^{-1}, which is equivalent to 7.824 Gy h^{-1}.

References

[1] L.H. Johnson and D.W. Shoesmith, in: Radioactive Waste Forms for the Future, eds. W. Lutze and R.C. Ewing (Elsevier Science, Amsterdam, 1988) p. 635.
[2] S. Sunder, G.D. Boyer and N.H. Miller. J. Nucl. Mater. 175 (1990) 163.
[3] S. Sunder, D.W. Shoesmith, H. Christensen, N.H. Miller and M.G. Bailey, Mater. Res. Soc. Symp. Proc. 176 (1990) 457.
[4] S. Sunder and D.W. Shoesmith, Atomic Energy of Canada Limited Report, AECL-10395 (1991).
[5] D.W. Shoesmith and S. Sunder, An Electrochemistry-based Model for the Dissolution of UO_2, Atomic Energy of Canada Limited Report, AECL-10488 (1991); SKB Technical Report, 91-63 (1991).
[6] R.S. Forsyth and L.O. Werme, J. Nucl. Mater. 190 (1992) 3.
[7] D.W. Shoesmith and S. Sunder, J. Nucl. Mater. 190 (1992) 20.
[8] W.J. Gray, H.R. Leider and S.A. Steward, J. Nucl. Mater. 190 (1992) 46.
[9] J. Bruno, I. Casas and A. Sandino, J. Nucl. Mater. 190 (1992) 61.
[10] K. Ollila, J. Nucl. Mater. 190 (1992) 70.
[11] S. Sunder, D.W. Shoesmith, H. Christensen and N.H. Miller, J. Nucl. Mater. 190 (1992) 78.
[12] L.H. Johnson, D.M. Leneveu, D.W. Shoesmith, D.W. Oscarson, M.N. Gray, R.J. Lemire and N.C. Garisto, The disposal of Canada's Nuclear Fuel Waste: The Vault Model for Postclosure Assessment, Atomic Energy of Canada Limited Report, AECL-10714 (1994).

[13] L.H. Johnson, J.C. Tait, D.W. Shoesmith, J.L. Crosthwaite and M.N. Gray, The disposal of Canada's Nuclear Waste: Engineered Barriers Alternatives, Atomic Energy of Canada Limited Report, AECL-10718 (1994).
[14] B. Grambow, A. Loida, P. Dressler, H. Geckeis, P. Diaz, J. Gago, I. Cassas, J. de Pablo, J. Gimenes and M.E. Torrero, Long-term Safety of Radioactive Waste Disposal: Reaction of High Burnup Spent Fuel and UO_2 in Saline Brines at Room Temperature (Kernforschungszentrum, Karlsruhe, KfK 5377, 1994).
[15] D.W. Shoesmith, S. Sunder and W.H. Hocking, in: Electrochemistry of Novel Materials, eds. J. Lipkowski and P.N. Ross (VCH, New York, 1994) p. 297.
[16] G.A. Parks and D.C. Pohl, Geochim. Cosmochim. Acta 52 (1988) 863.
[17] R.J. Lemire and F. Garisto, The Solubility of U, Nb, Pu, Th and Tc in a Geological Disposal Vault for Used Nuclear Fuel, Atomic Energy of Canada Limited Report, AECL-10009 (1989).
[18] M. Gascoyne and D.C. Kamineni, Groundwater Chemistry and Fracture Mineralogy in the Whiteshell Research Area: Supporting Data for the Geosphere and Biosphere Transport Models, Technical Record, Whiteshell Laboratories, Atomic Energy of Canada Limited Report, TR-516 (1992).
[19] M. Kolar and F. King, Mater. Res. Soc. Symp. Proc. (1996) in press.
[20] H.J. Smith, J.C. Tait and R.E. Von Massow, Radioactive Decay Properties of Bruce A CANDU^{TM} UO_2 Fuel and Recycle Waste. Atomic Energy of Canada Limited Report, AECL-9072 (1987).
[21] S. Sunder, Alpha, beta and gamma dose rates in water in contact with used CANDU UO_2 Fuel, Atomic Energy of Canada Limited Report. AECL-11380 (1995).
[22] S. Sunder, D.W. Shoesmith, H. Christensen, M.G. Bailey and N. Miller. Mater. Res. Soc. Symp. Proc. 127 (1989) 317.
[23] J.W.T. Spinks and R.J. Woods, An Introduction to Radiation Chemistry, 3rd Ed. (Wiley-Interscience, New York, 1990).
[24] M.G. Bailey, L.H. Johnson and D.W. Shoesmith, Corros. Sci. 25 (1985) 233.
[25] D.W. Shoesmith, B.M. Ikeda, F. King and S. Sunder, in: NACE Book Life Predictions of Structures Subjected to Environmental Degradation; Corrosion'96, Denver, Mar. 24–29 (1996) p. 101.
[26] S. Sunder, D.W. Shoesmith, M.G. Bailey, F.W. Stanchell and N.S. McIntyre, J. Electroanal. Chem. 130 (1981) 163.
[27] N.S. McIntyre, S. Sunder, D.W. Shoesmith and F.W. Stanchell, J. Vac. Sci. Technol. 18 (1981) 714.
[28] J.D. Rudnicki, R. Russo and D.W. Shoesmith, J. Electroanal. Chem. 372 (1994) 63.
[29] D.W. Shoesmith, S. Sunder, M.G. Bailey and G.J. Wallace, Corros. Sci. 29 (1989) 1115.
[30] S. Sunder, D.W. Shoesmith, R.J. Lemire, M.G. Bailey and G.J. Wallace, Corros. Sci. 32 (1991) 373.
[31] S. Sunder, D.W. Shoesmith and N.H. Miller, Mater. Res. Soc. Symp. Proc. 294 (1993) 36.
[32] S. Sunder, D.W. Shoesmith, N.H. Miller and G.J. Wallace, Mater. Res. Soc. Symp. Proc. 257 (1992) 345.
[33] P. Taylor, D.D. Wood and A.M. Duclos, J. Nucl. Mater. 189 (1992) 116.
[34] S. Sunder and N.H. Miller, XPS, XRD and SEM study of UO_2 by Air in Gamma Radiation at 150°C, Atomic Energy of Canada Limited Report, AECL-111351 (1995).
[35] D.W. Shoesmith, S. Sunder, L.H. Johnson and M.G. Bailey, Mater. Res. Soc. Symp. Proc. 50 (1985) 309.
[36] R.C. Weast, ed., CRC Handbook of Chemistry and Physics (CRC, Boca Raton, FL, 1969).
[37] S. Sunder, D.W. Shoesmith, L.H. Johnson, G.J. Wallace, M.G. Bailey and A.P. Snaglewski, Mater. Res. Soc. Symp. Proc. 84 (1987) 103.
[38] H. Christensen and S. Sunder, J. Nucl Mater. 238 (1996) 70.
[39] H. Christensen, S. Sunder and D.W. Shoesmith, Calculation of Radiation Induced Dissolution of UO_2, Adjustment of the Model based on α-Radiolysis Experiments, Studsvik Material Report No. M-92/20 (Publ. Studsvik Material AB, Nykoping, Sweden, 1992).
[40] R. Vochen and E. De Grave, J. Nucl. Mater. 172 (1990) 241.
[41] T. Ingemansson and J. Elkert, Model for calculation of absorbed alpha and beta radiation dose to water in contact with highly burnt-up nuclear fuel, ABA Atom Report, Asea Brown Boveri, Sweden, RM-91-23 (1991).
[42] L.O. Werme and J.P. Sato, Mater. Res. Soc. Symp. Proc. 212 (1990) 343.
[43] L.O. Werme, P. Sellin and N. Kjellbert, Copper canisters for nuclear high level waste disposal, Corrosion aspects, Swedish Nuclear Fuel and Waste Management Company Technical Report, TR-92-26 (1992).
[44] J.C. Wren, D.W. Shoesmith and S. Sunder, unpublished work.
[45] M.P. Lahalle, J.C. Krupa, R. Guillaumont, M. Genet, G.C. Allen and N. Holmes, Mater. Res. Soc. Symp. Proc. 127 (1989) 351.
[46] D.W. Shoesmith, J.C. Tait, S. Sunder, W.J. Gray, S.A. Steward, R.E. Russo and J.D. Rudnicki, Factors Affecting the Differences in Reactivity and Dissolution Rates Between UO_2 and Spent Nuclear Fuel, Atomic Energy of Canada Limited Report, AECL-11515 (1996).
[47] D.J. Wronkiewicz, J.K. Bates, T.J. Gerding, E. Veleckis and B.S. Tani, J. Nucl. Mater. 190 (1992) 107.
[48] SKB, Final disposal of Spent Nuclear Fuel, Importance of the bed rock safety SKB Sweden, Technical Report TR-92-20 (1992).
[49] S. Sunder, G.D. Boyer and N.H. Miller, J. Nucl. Mater. 175 (1990) 163.
[50] T.E. Eriksen, U.B. Eklund, L. Werme and J. Bruno, J. Nucl. Mater. 227 (1995) 76.